Submitted May 15, 2009; accepted July 20, 2009. Reference No. ST115 ; Category 2, 5.
See also P. Odier et al., Supercond. Sci. Technol. 22, 125024

Coated Conductors on Tubular Metallic Wires by Combined Chemical Approaches

C. Millon[1,2], S. Morlens[1], P. Chaudoüet[2], C. Jimenez[2], J.L. Soubeyroux[1], P. Tixador[1], A. Allais[3], C. F. Theune[4], P. Odier[1]

[1] Institut Néel and CRETA, CNRS&UJF, 25 av des martyrs, BP 166, 38042 Grenoble cedex 09, France.

[2] LMGP CNRS UMR5628- Grenoble INP –Minatec, 3 parvis Louis Néel, BP 257, 38016 Grenoble, France.

[3] Nexans Research Centre, 170, avenue Jean Jaurès, 69353 Lyon Cedex 07, France.

[4] Nexans Deutschland Industry – Hannover

Corresponding author: philippe.odier@grenoble.cnrs.fr

Abstract **- Fabrication of YBCO wires has been explored by using tubes formed from textured tapes. The texture of tubes made from Ni-5 at % W is characterized as a bi-axial texture developing along both the axis and the circumference of the cylinder. The deposition of a buffer layer by metal-organic deposition on such a tube is described with the practical example of $La_2Zr_2O_7$. A superconducting YBCO layer is deposited on top; its texture and the electrical performance are evaluated. In the present state of the art, the YBCO is superconducting at 88 K; it is textured, but can carry only week supercurrents due to insufficient percolation paths. Improvements of the process are underway to enhance the transport current properties.**

Submitted May 15, 2009; accepted July 20, 2009. Reference No. ST115 ; Category 2, 5.

Keywords **- YBCO, HTS wire, coated conductor, tubular conductor, textured tube, $La_2Zr_2O_7$, LZO**

I. INTRODUCTION

Coated conductors (CCs) inspire considerable research efforts in the field of applied superconductivity. Researchers are aiming to replace the first generation of high-T_c superconducting (HTS) wires, the physical properties of which are limited, by CCs. The second generation of high-T_c wires (CC 2G) consists of a thin layer of an $YBa_2Cu_3O_{7-\delta}$ (YBCO) deposit, bi-axially textured, on similarly textured buffer layers deposited on a metallic substrate. The crucial role of these buffers is to adapt the structure of YBCO to that of the substrate and to protect the metal from oxidation during the process of deposition. An economic substrate is a flat and thin metallic tape prepared by a Rolling-Assisted Bi-axially Textured (RABiT) process. Excellent substrates are also

obtained by a more complex route using Ion Beam Assisted Deposition (IBAD) [1]. Such CCs tapes with very high performance over long conductor lengths are fabricated by various approaches [2-4]. Nexans and Bruker HTS, collaborating within a European consortium involving industry and academia, announced recently the successful tests of a 30 m CC 2G cable able to carry 17 MW. The CC were processed by physical deposition techniques (Pulsed Laser Deposition, PLD, and IBAD) [5]. IGC-Superpower Inc (USA) [2] uses a complex combination of physical deposition techniques on IBAD and Metal Organic Chemical Vapour Deposition (MOCVD) to deposit the YBCO layer. AMSC (USA) uses a Metal Organic Deposition (MOD) approach with trifluoroacetates (TFA) to deposit YBCO on top of a complex architecture of buffer layers obtained by physical methods [6]. Currently, using the most advanced technology, one can produce 600-m-long sections of tape, 4 mm in width, with a critical current I_c = 80 A to 100 A at 77K. All these conductors are flat tapes. This geometry has obvious drawbacks for conductors and cables using a cylindrical geometry. This is why J. Schwartz, referring to the problems of anisotropy in superconducting tapes, said during a plenary talk at MT20 at Philadelphia 2008: "A YBCO round wire technology would be the holy grail…".

Nexans, in collaboration with academic research groups in Grenoble (France) is developing a new type of HTS conductor where a flat metallic substrate is shaped into a longitudinally-laser-welded tube. The benefits of a round conductor for electrical engineering are straightforward. One major advantage is the use of generic engineering and manufacturing tools. The conductor will be composed of several such tubes assembled together in a cylindrical geometry. The idea emerged from the association of the research on sol-gel based REBCO coated conductors at Nexans SuperConductors (Hürth-Germany) and the laser welding technology developed at Nexans Hannover (Germany) to produce tubes from thin metallic sheets [7]. This could lead to a breakthrough for the HTS cable system, where the efficient use of concentric cylindrical CC 2G tubes would allow one to significantly lower the performance threshold for HTS material: instead of 30 A/mm for the flat tape at 77K, a level of 5 A/mm of circumference would be sufficient to manufacture a high-power transmission cable.

In this paper, we present our first attempts to process such round superconducting tube conductors. The problem was, first, to identify the texture of the substrate, and then to cover it effici ently with a simple architecture of layers. We choose a layer of $La_2Zr_2O_7$ (LZO) deposited by MOD and covered by YBCO using MOCVD, a combination recently proven to be a good alternative [8]. The YBCO layer was shown to be textured and superconductive, although the process is not yet optimised to result in high critical current.

II. EXPERIMENTAL

A. Substrate preparation

Textured tapes were rolled and welded (RW) at Nexans (Hannover, Germany) in the shape of small diameter tubes according to a patented process [7]. The tubes had a diameter of 1.8 mm and a wall thickness of 80 µm. We have investigated tubes rolled from Ni-5 at% W tapes as delivered by EVICO (Dresden, Germany) and tubes rolled from tapes which were MOD-coated with a thin layer of LZO according to a process developed at Nexans (Hürth, Germany) [9].

B. X- ray characterization, EBSD, SEM

X-ray diffractograms were recorded using a diffractometer designed for studies of textured films. The apparatus was a four-circle diffractometer from Seifert (Germany), type MZ IV, equipped with multilayer optics from Xenocs (France), and using the Shultz configuration (with a horizontal angular acceptance of the detector equal to 0.06°). The wavelength was that of the Cu-K_α radiation. The detector is behind a graphite monochromator. Small pieces (5 mm in length) of tubes were pressed under 5 MPa into a flat rectangular shape for diffraction measurements. Electron Back Scattered Diffraction (EBSD) was performed with a Zeiss Ultra 500 directly on the tubes. The small area probed by this technique (~ 600 μm^2) allows considering its surface quasi flat. Secondary Electron Microscopy (SEM) was made on the same tubes.

C. LZO deposition on tubes

A propionate solution of La and Zr was prepared according to a method described elsewhere [10]. The concentration was low enough (0.3 mol/l per element) to be in the solubility range of the solution. The tubes were ultrasonically cleaned in acetone and then in isopropanol during 10 min. The deposition was performed in a glove box to work under constant humidity and to avoid dust pollution. The samples (5 cm long) were dipped into the solution for 30 s and withdrawn at a speed of 60 mm/min, the deposit was then dried at 60 to 80 °C using infrared lamps during 60 s inside the glove box. This way, polymeric films of La-Zr propionate mix were formed on the tubes.

D. Crystallization

The tubes were put in an alumina boat and inserted into a furnace under Ar - 5% H_2 gas flow (10-50 l/h). The deposit was then heated with a one ramped step up to 960°C; it was then hold during 30 min at that temperature [8]. Cooling to room temperature was performed at the same rate.

E. MOCVD

Tubes with the LZO buffer layer have been covered with YBCO using MOCVD in an apparatus developed earlier [11, 12]. This system consists of a pressurized liquid precursor source and an injector which controls accurately the amount of precursors introduced. The liquid precursor is flash evaporated at 280°C under low pressure (6.7 Pa). This liquid precursor is a metal-organic solution containing a mixture of $Y(tmhd)_3$, $Ba(tmhd)_2$ and $Cu(tmhd)_2$ (tmhd = 2,2,6,6-tetramethyl-3,5-heptanedionate) dissolved in monoglyme with the appropriate molar ratio. The deposition takes place on the tube at 800°C in a resistively heated chamber under a controlled atmosphere (60% Ar + 40% O_2), at a reduced pressure of 0.6 kPa. After deposition, the substrate was oxygenated at 500°C under 0.8 kPa of pure oxygen during one hour. A 350 nm thick silver layer was then thermally evaporated on the YBCO layer as a shunt.

III. RESULTS

A. Tube texture and stability

A tube made from a textured tape by RW processing was characterized by x-ray diffraction. In Figure1 (a), which shows the θ-2θ scan, the dominant (200) reflexion (at $2\theta = 51.54°$) and the very weak (111) and (220) peaks points to a cube texture of the Ni substrate with the content of W in the range 4 to 5 at% (lattice parameter $a = 3.543$ Å). The cube texture was confirmed by measuring rocking curves (ω scans, FWHM = 8. 3°), such as that in Figure1 (b), and (111) ϕ -scans (FWHM = 7.8°) with an example shown in Figure1 (c). The misalignment between grains (out-of-plane and in-plane) was slightly enhanced (15-20%) with respect to the initial tape [see the ω scan of Figure 1 (e)] for two reasons: (i) the rolling induced a stretching deformation of the outer surface of the tape and additional misalignments between grains; (ii) the tubes were flattened for performing x-ray measurements. Rolling a textured tape to tubular shape induces an additional small misalignment of ~ 0.4°/grain in the radial direction for a tape of 6 mm width and a grain size of 50 μm. The same effect occurs when a tube is flattened for measurements. A schematic representation of the tube microstructure is drawn in Figure 1 (d). It is composed of cubes aligned along the axis of the tube and also along the circumference of the cylinder; this differs from a fibre texture where only one direction of alignment is fixed.

After the RW process, the surface of the tube is smooth on a scale of 100 μm, as shown by the low-magnification SEM image of Figure 2 (a), but higher magnification of Figure 2 (b) evidences lines inclined at 45° of the tube axis and crossing each other perpendicularly. Such lines did not appear extensively in the initial tape, and must have been generated during the rolling process. More precisely, referring to a neutral fibre at the middle of the tube wall, the generated strain ε amounts to:

$$\varepsilon = e/(D-e), \qquad (1)$$

where e is the thickness of the tube and D its outer diameter. Typically, a tape with a thickness of 80 μm when rolled into a tube of 1.8 mm will induce a strain of 4.6 % which is sufficient to exceed the elastic range of metal deformation. This strain is relaxed due to the formation of Lüders bands [13], which are the lines visible in Figure 2 (b). The Lüders bands have another interesting effect on the size of the crystallites. The grain size in the initial tape was ~20- 50 μm; such large grain size induces a marked fine structure in the rocking curve, Figure1 (e), because the number of grains probed in the irradiated area is rather small (about 20 grains in the width of the irradiated area). After the shaping into tubes, the elementary crystallite size is reduced to approximately 0.2 μm in the Lüders bands and sampling encompasses now a very large number of crystallites. Consequently, no marked fine structure is observed in the rocking curve of the tube, Figure1 (b).

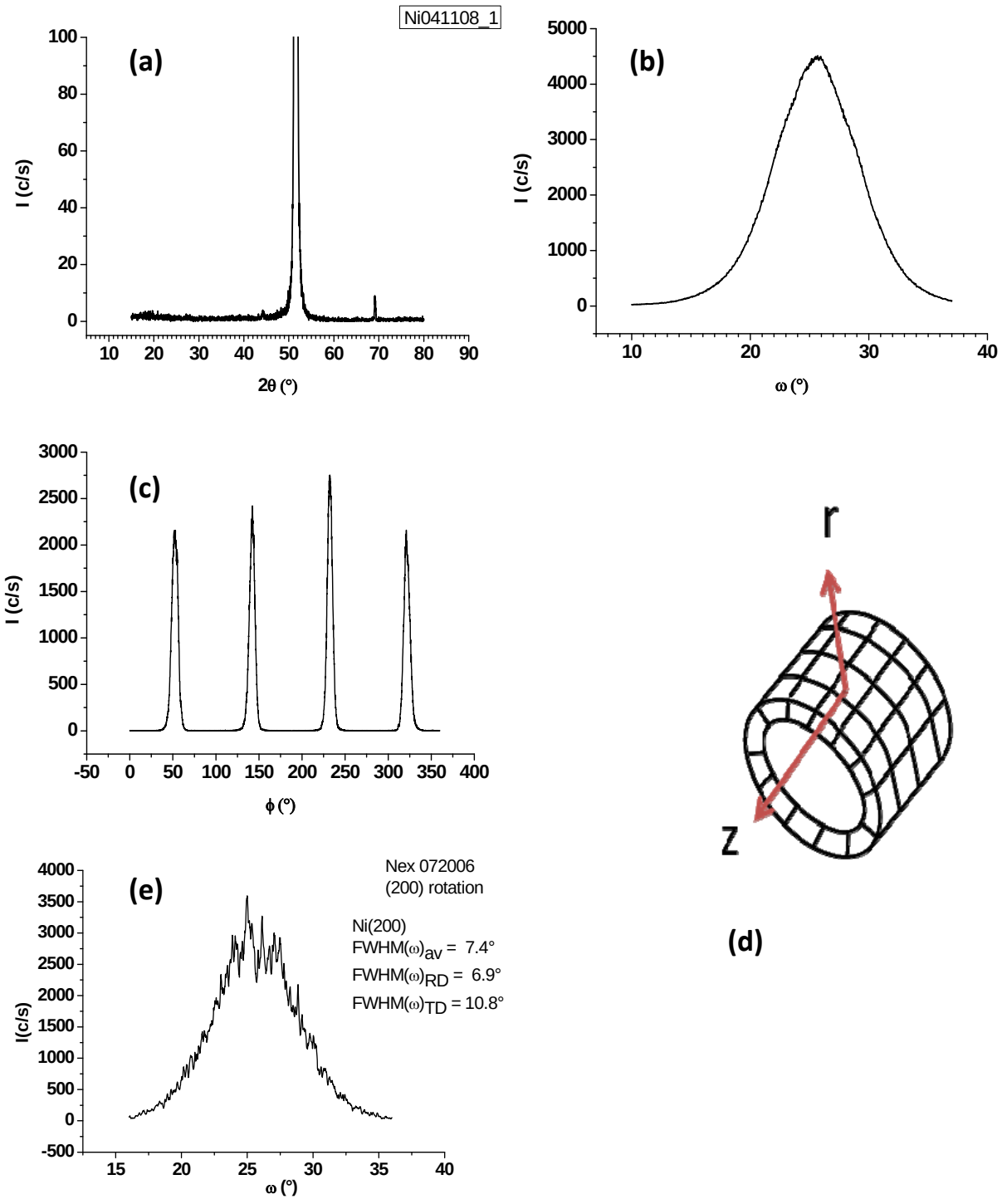

Fig. 1. Texture of a tube after the RW process: (a) θ- 2θ scan; (b) ω-scan of (200); (c) ϕ scan of (111); (d) schematic of the texture; (e) ω-scan of the initial tape. The peak at 69° of Fig.1(a) originates from the substrate.

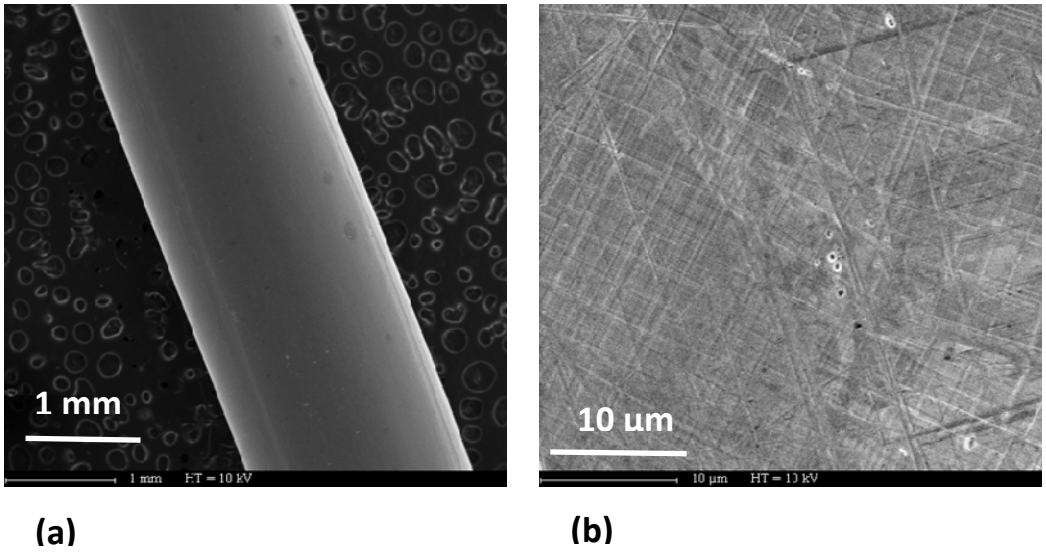

Fig. 2. SEM image of a rolled-welded tube. 2 (a): x 50; 2 b): x 5000. Crossing lines are Lüders bands.

Such a tube has been covered with a layer of LZO precursor and heated for its crystallization as described in Section II.D. The analysis of the LZO layer will be reported below (see discussion) while we focus here on the substrate. Phi-scans of the diffraction by (111) planes of the Ni -5 at % W evidence a strong recrystallization of the substrate, as seen in Figure 3 (a). This is consistent with the intensity increase of the (111) reflection observed by θ-2θ scan (at 44.46°) that was absent prior to the annealing, and with the reduction of the (200) reflection compared with the initial sample. The θ-2θ scan is shown in Figure 3 (b). This experiment proves a degraded stability of tubes formed from textured tapes and could be a severe limitation to the use of this processing.

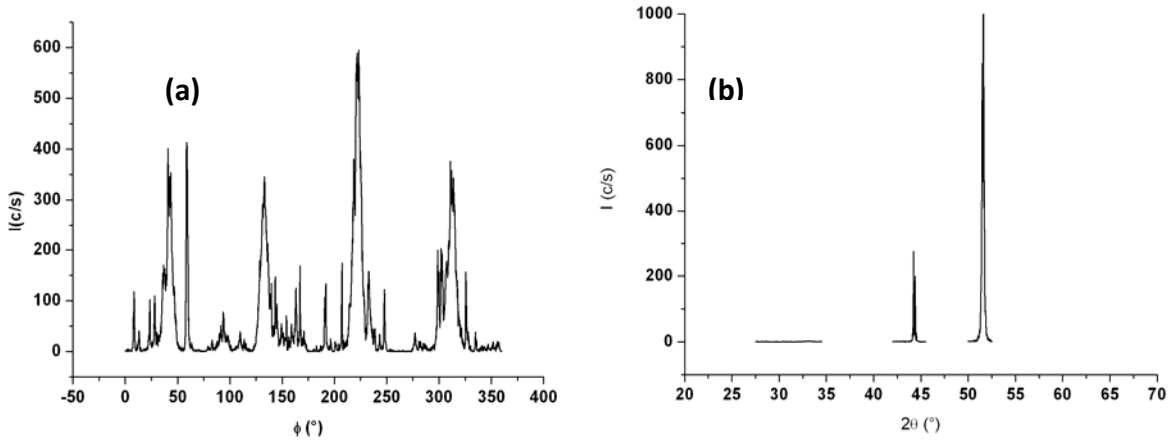

Fig. 3. Recrystallization of a Ni-5at%W tube after the RW process and annealing at 960°C: (a): phi-scan of (111); (b): θ- 2θ scan.

B. LZO and YBCO texturing on tubes

To evaluate experimentally another route of processing, one tube was RW with a LZO layer already deposited on its surface. This layer was made according to the procedure described in reference [9] and SEM inspection did not reveal cracks or pores at the micron scale. However, it contained nanopores often observed in such MOD layers [14]. The LZO layer was biaxially textured up to its surface according to EBSD characterization (not shown here). Typical mosaicity was in the range of 7° - 8° both for in-plane and out-of-plane. After RW, the LZO layer was severely degraded, in effect the tube was stretched during its pulling and forced to pass through a die to rectify the welded zone. Figure 4 (a) shows the SEM image of the tube surface, while its EBSD map is shown in Figure 4 (b); in contrast to X-ray, EBSD could be made directly on the tube. The SEM evidences many fractures in the LZO layer.

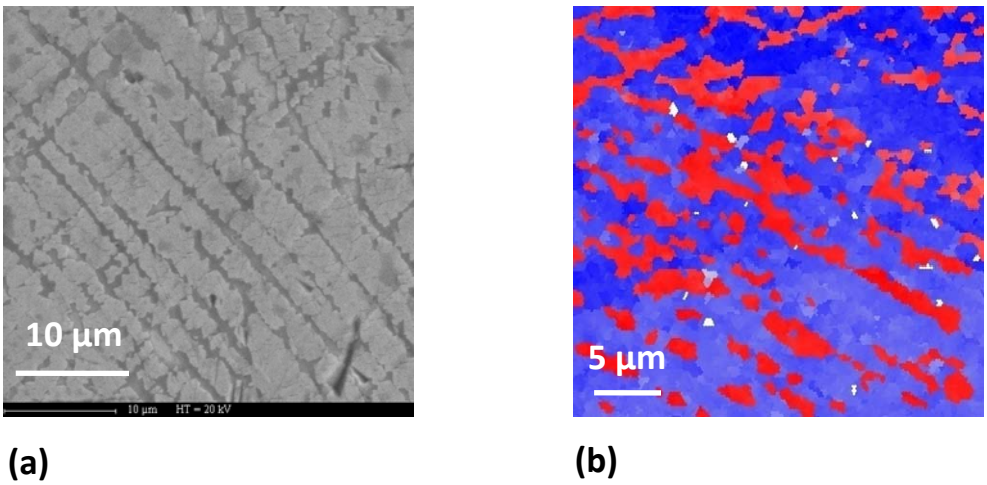

Fig. 4. Fractured LZO layer after the RW process. 4a: SEM of a RW tube where the initial tape was covered with LZO deposited by MOD process; 4b: EBSD of the same area, the red encoded areas correspond to Ni which crystal directions are rotated 45° from that of the LZO in blue.

This oxide is hard and fragile, like a ceramic, and pulling of the Ni-W substrate induced cracks and expunged LZO parts. These fractures follow lines oriented at ~ 45° to the pulling direction corresponding to Lüders bands [13] in the substrate. The expunged parts made the Ni visible; these portions can contribute to the same diffracted pattern than that of LZO because both have similar lattice parameters (considering the reduced unit cell). However, the LZO crystals directions are rotated by 45° from those of the Ni-5 at% W when LZO heteroepitaxially grows on the Ni grains [8], hence the fractured zone should show a lattice rotated by 45° from the zones covered by LZO. Figure 4 (b) shows this effect: the red contour coding indicates crystalline directions rotated by 45° from the blue areas; they correspond to the Ni-5 at% W parts exposed after expunging the LZO. It is interesting to notice that these areas correspond exactly to the fractures evidenced by SEM of Figure4 (a). Therefore, the surface of these tubes is not appropriate to deposit a smooth and homogeneous YBCO layer.

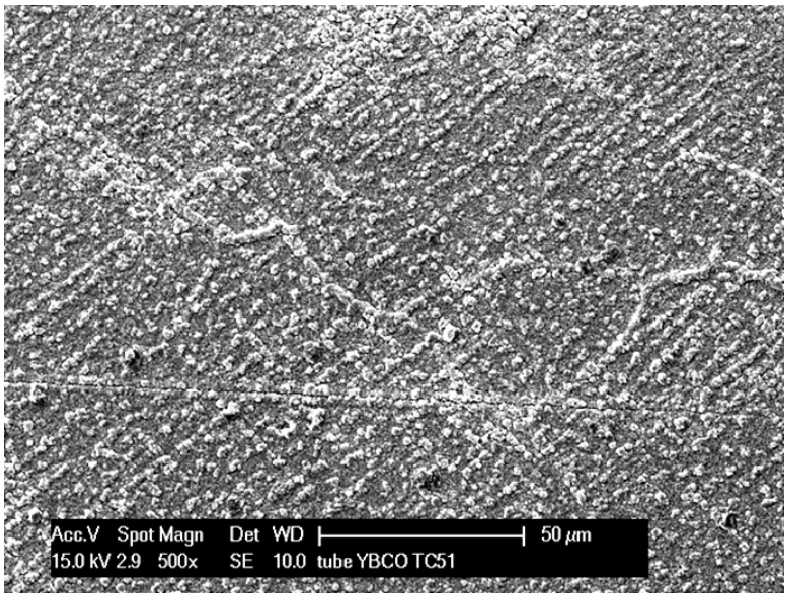

Fig. 5. SEM of the YBCO deposit on a RW tube with a fractured LZO buffer. YBCO forms out-growth at the places where the LZO is fractured.

Figure 5 shows a YBCO deposit made by MOCVD on such a surface, evidencing accumulation of "powder like" particles along the fractures of the LZO film. No superconductivity was observed in this film, probably because of the contamination by Ni and/or no effective percolation paths between the YBCO parts.

The whole LZO surface was then covered by a second coating of LZO by means of MOD process; the goal of this second coating was to heal the damaged surface. X-ray showed a textured LZO with signals increasing with thickness. EBSD has been carried out to check whether the surface layer was textured or not. Figure 6 shows an orientation map with a blue color encoding for <100> directions. Note that more that 90 % of the grains probed have a direction within 0° and 10° from the <100> direction. In addition, comparing to Figure 4, the uncovered areas have been clearly reduced.

The surface state of the healed LZO layer of this tube was good enough to enable a better YBCO quality. A 500 nm thick YBCO film was then deposited by MOCVD and covered with a silver shunt. The resistance R of two such tubes processed in a similar way has been measured in He gas from room temperature down to 40 K. The $R(T)$ evidenced a superconducting phase at 73 K for tube number 1 and 88 K for tube number 2, with broad transitions (ΔT = 7.5 K for tube number 1 and ΔT = 8 K for tube number 2) shown in Figure 7. We attribute this rather low T_c and broad transition to the diffusion of Ni, NiO or W into the YBCO not fully protected by the LZO layer. Tube number 2 was measured down to liquid He temperature and only a low superconducting current passed through the sample.

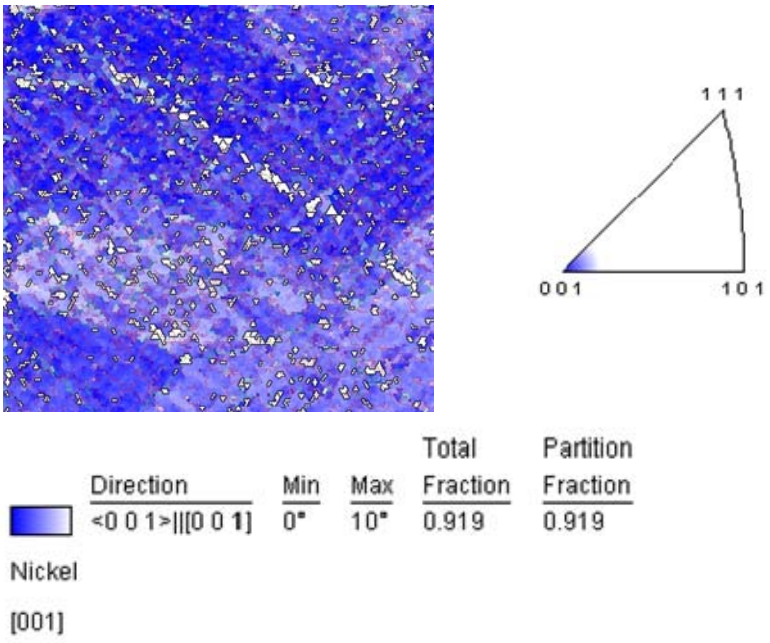

Fig. 6. EBSD of a tube after a second LZO coating.

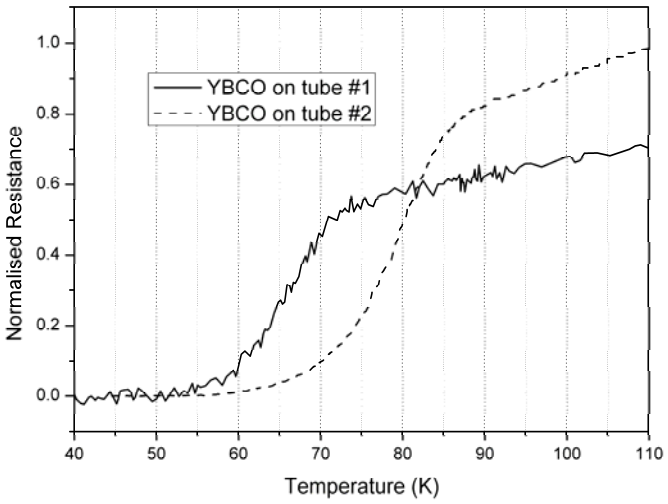

Fig. 7. Transport properties of YBCO textured tubes.

An x-ray measurement was performed after removing the silver shunt and after flattening a small portion of the tube (7 mm). Figure 8 shows a θ-2θ scan evidencing YBCO (00l) reflections and other reflections due to Ni (200), LZO(004), $NiWO_4$, and NiO. $NiWO_4$ (and NiO) have been grown during the YBCO deposition which was performed under an oxygen partial pressure of 0.6 kPa at 800°C, instructive of an insufficient protection of the metallic part by LZO. However, the only (00l) reflections suggest a cube textured YBCO that has been confirmed by rocking-curve and phi-scan measurements on the (102) line, with unfortunately a weak acuity of the texture, partly due to the flattening of the tube for the measurement.

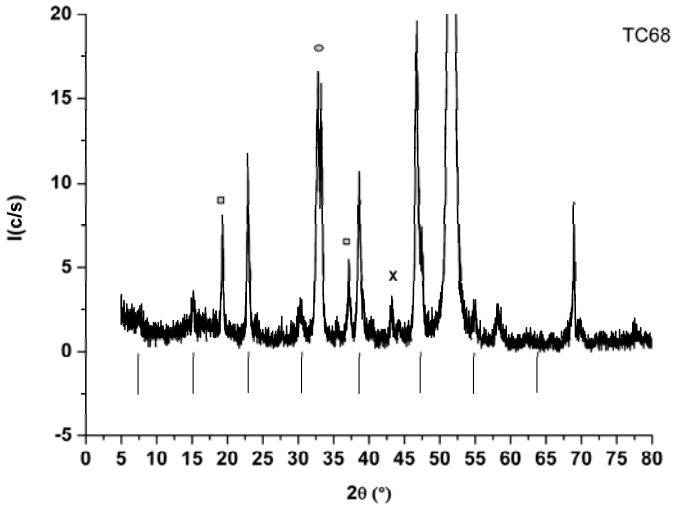

Fig. 8. X-ray scan of a healed tube covered with YBCO by MOCVD. Lines points to YBCO(00l). Secondary phases are NiWO4 (□), LZO (0) and NiO (x). The largest peak observed at $2\theta = 51.61°$is due to Ni(200), suggesting a smaller W content than 5 at%.

IV. DISCUSSION

In the process described here, and more generally in those involving RABiTS, the texture is transferred from the substrate to the buffer layer (here LZO) by epitaxial growth on the grains of the Ni. The stability of the substrate texture is then, *a priori*, a crucial factor for the textured tubes presented here. If the tubes are made from textured tapes, the rolling into the tubular shape puts new strain energy in the metal sheet that may induce secondary recrystallization after the second annealing, with a subsequent modification of the texture. We hope that optimization of the process by using the effect of skin-pass [15] could avoid these drawbacks. However, despite the recrystallization of the Ni during the heat treatment, we were able to texture the deposited LZO with the typical cube texture. Therefore, the nucleation of LZO occurs at a temperature lower than that of the recrystallization of the substrate, thus providing a small window for the process.

When using LZO covered tapes, the first LZO layer was severely cracked during the process used to shape the tube. We have attempted to heal these zones by a second coating and observed that the cracks are filled with the second LZO deposition. EBSD measurements have shown an improvement of the surface texture, also confirmed by better superconducting properties of the YBCO deposited on this surface. However, some deficient surface areas remain and more structural characterizations are needed to fully determine the texture of these areas.

The YBCO layer covers parts of the tube surface, because the MOCVD apparatus was not designed for round substrates. Simulation using “fluent 6.2” software has shown that only 1/3 of the tube circumference was effectively covered by YBCO and this fact has been confirmed by an EDS study. The deposited YBCO layer was textured as demonstrated by x-ray data. It is presumed, however, that the deficient areas (mentioned above) will be an obstacle to the superconducting current percolation. The YBCO has shown a superconducting behavior but with a broad transition certainly resulting from impurities that could have diffused trough the buffer

layer, probably through the defective areas. Only a small critical current has been measured for this YBCO layer at low *T* as a consequence of the only partly covered surface of the tube and of the remaining defective areas. It is known that the quality of the LZO layer is crucial, especially in the case of the simple architecture used here [16], and we anticipate better results with improved LZO.

The texture of the substrate is transferred to the buffer layer and the YBCO layer by epitaxial growth on the grains of the substrate. At the beginning of this project, it was not obvious whether the angles between the grains would not increase by homothetic transfer. The present results tend to show that this is not the case; the misalignment between grains does not seem to increase drastically after several depositions. This is certainly due to smoothing the defects by the MOD process [8]. This is in contrast to physical methods operating under vacuum that would favor an exact copy of the support without any smoothing of defects.

V. CONCLUSION

Tubes of small diameter (1.8 mm) and thin wall thickness (80 μm) were prepared by technology developed at Nexans and applied to RABiTs tapes. These tubes have a textured structure along the axial direction but also along the radial direction. Such tubes can be protected by a textured buffer layer made from lanthanum zirconate, $La_2Zr_2O_7$, on which YBCO superconducting layer can be grown. In the actual process, the LZO layer is degraded and must be healed before superconducting YBCO layer is deposited by MOCVD. Presently, the onset of superconductivity in this YBCO layer is at 88 K. While the layer is textured, it can carry only week supercurrents due to insufficient percolation paths. Improvements of the process are underway to increase the transport current properties.

ACKNOWLEDGEMENTS

The authors wish to thank Dr. M. Rikel from Nexans Superconductor, Dr. C.E. Bruzek from Nexans-France, and Dr. T. Waeckerlé from AMSN for many helpful discussions. This work was financially supported by ANR French program Madisup, the European Union (FEDER) and the French Department for Industry (program FUI Superfact).

REFERENCES

[1] J.H. Durrell and N.A. Rutter, *Supercond. Sci. Technol*. **22,** 013001 (2009).
[2] V. Selvamanickam, Y. Chen, X. Xiong *et al*, *IEEE Trans. Appl. Supercond.* **17,** 3231 (2007).
[3] Y. Shioara *et al*, *Physica C* **445-448,** 496 (2006); M.W. Rupich et al, *IEEE Trans. Appl. Supercond.***17** 3379 (2007).
[4] A. Usoskin *et al*, *IEEE Trans. Appl. Supercond.* **17,** 3235 (2007).
[5] See for example http://www.reuters.com/article/pressRelease, March-2009 or ESNF Highlight HP18.
[6] A.P. Malozemoff, S. Fleshler, M. Rupich, *et al*., *Supercond. Sci. Technol.* **21,** 034005 (2008).
[7] A. Allais, D. Isfort, C.F. Theune, K. Porscher, Patents EP1916720 and US2008/0119365.
[8] T. Caroff, S. Morlens, A. Abrutis, *et al.*, *Supercond. Sci. Technol.* **21,** 75007 (2008).
[9] M.O. Rikel, D. Isforth, M. Klein, *et al*., *IEEE Trans. Appl. Supercond.*, Presentation 4MX03 of ASC (2008).
[10] Z.M. Yu, P. Odier, L. Ortega, *et al.*, *Mat.Sci. Eng. B*, **130,** 126 (2006).
[11] J.P. Senateur, F. Weiss, O. Thomas, R. Madar R, A. Abrutis, *Patent* 93/08838 PCT Fr94/00858.
[12] A. Abrutis, J.P. Sénateur, F. Weiss, *et al*., *Supercond. Sci. Technol.* **10,** 959 (1997).

[13] V.S. Anathan and E.O. Hall, *Acta Metall. Materialia*, **39,** 3153 (1991).
[14] C. Jiménez, T. Caroff, L. Rapenne, *et al.*, *J.Cryst.Growth*. **311,** 3204 (2009).
[15] S.W. Cheong, E.J. Hilinski, A.D. Rollett, *Metallurgical and Materials Transactions A*, **34A,** 1311 (2003).
[16] T. Caroff, L. Porcar, P. Chaudouët, *et al*., *IEEE Trans. Appl. Supercond.* **19**, No. 3 (2009) in press.